

# Rapidity evolution of Wilson lines at the next-to-leading order

Ian Balitsky

*Physics Dept., Old Dominion University, Norfolk VA 23529, and  
Theory Group, Jlab, 12000 Jefferson Ave, Newport News, VA 23606\**

Giovanni A. Chirilli

*Department of Physics, The Ohio State University, Columbus, OH 43210, USA<sup>†</sup>*

(Dated: September 26, 2018)

At high energies particles move very fast so the proper degrees of freedom for the fast gluons moving along the straight lines are Wilson-line operators - infinite gauge factors ordered along the line. In the framework of operator expansion in Wilson lines the energy dependence of the amplitudes is determined by the rapidity evolution of Wilson lines. We present the next-to-leading order hierarchy of the evolution equations for Wilson-line operators.

PACS numbers: 12.38.Bx, 12.38.Cy

## I. INTRODUCTION

One of the most successful approaches to high-energy scattering is the operator expansion in Wilson lines. (For a review, see Refs. [1, 2]). This approach is based on factorization in rapidity [3] and the cornerstone of the method is the evolution of Wilson-line operators with respect to their rapidity. The most well-studied part is the evolution of the “color dipole” (the trace of two Wilson lines) which has a great number of phenomenological applications. The evolution of color dipoles is known both in the leading order (the BK equation [4, 5]) and in the next-to-leading order (NLO) [6, 7] and the solutions of the BK with running  $\alpha_s$  [8, 9] are widely used for  $pA$  and heavy-ion experiments at LHC and RHIC. However, recently it was realized that many interesting processes are described by the evolution of more complicated operators such as “color quadrupoles” (trace of four Wilson lines) [10]. To describe such evolution the NLO BK must be generalized to the full hierarchy of Wilson-lines evolution which is the topic of the present paper. We were following the method of calculation developed in Ref. [6] and the results for many diagrams (with the notable exception of “triple interaction” diagrams) can be taken from that paper. In this letter-type publication we present only the final results for the kernels and leave the details of calculation for future paper(s).

## II. HIGH-ENERGY OPE AND RAPIDITY FACTORIZATION

Consider an arbitrary Feynman diagram for scattering of two particles with momenta  $p_A = p_1 + \frac{p_A^2}{s} p_2$  and  $p_B = p_2 + \frac{p_B^2}{s} p_1$  ( $p_1^2 = p_2^2 = 0$ ). Following standard

high-energy OPE logic we introduce the rapidity divide  $\eta$  which separates the “fast” gluons from the “slow” ones. As a first step, we integrate over gluons with rapidities  $Y > \eta$  and leave the integration over  $Y < \eta$  to be performed afterwards. It is convenient to use the background field formalism: we integrate over gluons with  $\alpha > \sigma = e^\eta$  and leave gluons with  $\alpha < \sigma$  as a background field, to be integrated over later. Since the rapidities of the background gluons are very different from the rapidities of gluons in our Feynman diagrams, the background field can be taken in the form of a shock wave due to the Lorentz contraction. The integrals over gluons with rapidities  $Y > \eta$  give the so-called impact factors -coefficients in front of Wilson-line operators with the upper rapidity cutoff  $\eta$  for emitted gluons. The Wilson lines are defined as

$$U_x^\eta = \text{Pexp} \left[ ig \int_{-\infty}^{\infty} du p_1^\mu A_\mu^\sigma(ux_\perp + x_\perp) \right],$$

$$A_\mu^\eta(x) = \int d^4k \theta(e^\eta - |\alpha_k|) e^{ik \cdot x} A_\mu(k) \quad (1)$$

where  $\alpha$  is Sudakov variable ( $p = \alpha p_1 + \beta p_2 + p_\perp$ ).

The result for the amplitude can be written as

$$A(p_A, p_B) = \sum I_i(p_A, p_B, z_1, \dots, z_n; \eta) \langle p_B | U^\eta(z_1) \dots U^{\dagger\eta}(z_n) | p_B \rangle \quad (2)$$

where the color indices of Wilson lines are convoluted in a colorless way (and connected by gauge links at infinity). As in usual OPE, the coefficient functions (“impact factors”  $I_i$ ) and matrix elements depend on the “rapidity divide”  $\eta$  but this dependence is cancelled in the sum (2). It is convenient to define the impact factors in an energy-independent way (see e.g. [11]) so all the energy dependence is shifted to the evolution of Wilson lines in the r.h.s. of Eq. (2) with respect to  $\eta$ .

To find the evolution equations of these Wilson line operators with respect to rapidity cutoff  $\eta$  we again factorize in rapidity. We consider the matrix element of the set of Wilson lines between (arbitrary) target states and integrate over the gluons with rapidity  $\eta_1 > \eta > \eta_2 = \eta_1 - \Delta\eta$

\*Electronic address: balitsky@jlab.org

<sup>†</sup>Electronic address: chirilli.1@asc.ohio-state.edu

leaving the gluons with  $\eta < \eta_2$  as a background field (to be integrated over later). In the frame of gluons with  $\eta \sim \eta_1$  the fields with  $\eta < \eta_2$  shrink to a pancake and we obtain four diagrams of the type shown in Fig. 1. The result of the evolution of Wilson lines can be presented as infinite hierarchy of evolution equations for n-Wilson-line operators. This hierarchy of equations can be constructed from finite number of “blocks” with this number equal to the order of perturbation theory.

It should be mentioned that an alternative approach to high-energy scattering in the dense QCD regime is to write the rapidity evolution of the wavefunction of the target which is governed by the JIMWLK equation [12]. The one-loop evolution of the JIMWLK Hamiltonian summarizes the hierarchy of equations presented in the next Section. (After completion of this paper we have learned about the paper [13] where NLO JIMWLK Hamiltonian is presented.)

### III. LO HIERARCHY

In the leading order the hierarchy can be built from self-interaction (evolution of one Wilson line) and “pairwise interaction”. The typical diagrams are shown in Fig. 1 and the equations have the form [4]

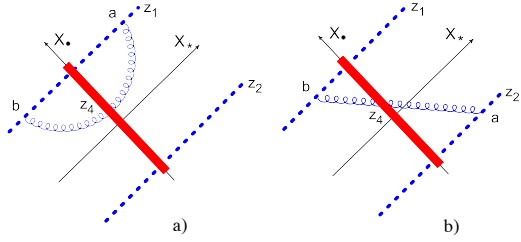


FIG. 1: LO diagrams.

$$\begin{aligned} \frac{d}{d\eta}(U_1)_{ij} &= \frac{\alpha_s}{\pi^2} \int \frac{d^2 z_4}{z_{14}^2} (U_4^{ab} - U_1^{ab})(t^a U_1 t^b)_{ij} \\ \frac{d}{d\eta}(U_1^\dagger)_{ij} &= \frac{\alpha_s}{\pi^2} \int \frac{d^2 z_4}{z_{14}^2} (U_4^{ab} - U_1^{ab})(t^b U_1^\dagger t^a)_{ij} \end{aligned} \quad (3)$$

for the self-interaction diagrams of Fig. 1a type and

$$\begin{aligned} \frac{d}{d\eta}(U_1)_{ij}(U_2)_{kl} &= \frac{\alpha_s}{4\pi^2} \int d^2 z_4 [2U_4 - U_1 - U_2]^{ab} \\ &\times \frac{(z_{14}, z_{24})}{z_{14}^2 z_{24}^2} [(t^a U_1)_{ij}(U_2 t^b)_{kl} + (U_1 t^b)_{ij}(t^a U_2)_{kl}] \\ \frac{d}{d\eta}(U_1)_{ij}(U_2^\dagger)_{kl} &= -\frac{\alpha_s}{4\pi^2} \int d^2 z_4 [2U_4 - U_1 - U_2]^{ab} \\ &\times \frac{(z_{14}, z_{24})}{z_{14}^2 z_{24}^2} [(t^a U_1)_{ij}(t^b U_2^\dagger)_{kl} + (U_1 t^b)_{ij}(U_2^\dagger t^a)_{kl}] \\ \frac{d}{d\eta}(U_1^\dagger)_{ij}(U_2^\dagger)_{kl} &= \frac{\alpha_s}{4\pi^2} \int d^2 z_4 [2U_4 - U_1 - U_2]^{ab} \\ &\times \frac{(z_{14}, z_{24})}{z_{14}^2 z_{24}^2} [(U_1^\dagger t^a)_{ij}(t^b U_2^\dagger)_{kl} + (t^b U_1^\dagger)_{ij}(U_2^\dagger t^a)_{kl}] \end{aligned} \quad (4)$$

for the “pairwise” diagram shown in Fig. 1b. Hereafter we use the notation  $U_i \equiv U_{z_i}$  and the integration variable is called  $z_4$  for uniformity of notations in all Sections). All vectors  $z_i$  are two-dimensional and  $(z_i, z_j)$  is a scalar product.

The evolution equations in this form are correct both in the fundamental representation of Wilson lines where  $t^a = \lambda^a/2$  and in the adjoint representation where  $(t^a)_{bc} = -if^{abc}$ . In the adjoint representation  $U$  and  $U^\dagger$  are effectively the same matrices ( $U_{ab}^\dagger = U_{ba}$ ) so the three evolution equations (4) are obtained from each other by corresponding transpositions. (One should remember that  $(t^a)_{bc} = -(t^a)_{cb}$  in the adjoint representation). Since the color structure of the diagrams in the fundamental representation is fixed one can get the kernels by comparison with adjoint representation. Effectively, since our results will be always presented in the form universal for adjoint and fundamental representations the NLO results for the evolution of  $U \otimes U^\dagger$  and  $U^\dagger \otimes U^\dagger$  can be obtained by transposition.

### IV. NLO HIERARCHY

In the next-to-leading order (NLO) the hierarchy can be constructed from self-interactions, pairwise interactions, and triple interactions. The typical diagrams are shown in Fig. 2 ab, Fig. 2 cd, and Fig. 2 ef, respectively.

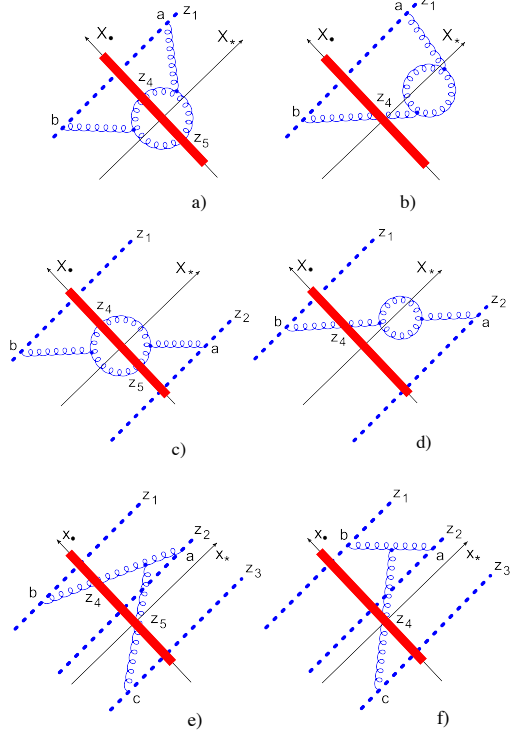


FIG. 2: Typical NLO diagrams.

### A. Self-interaction

The most simple part is the one-particle interaction (“gluon reggeization” term). The typical diagrams are shown in Fig. 2 a,b and the result has the form

$$\begin{aligned} \frac{d}{d\eta}(U_1)_{ij} &= \frac{\alpha_s^2}{8\pi^4} \int \frac{d^2 z_4 d^2 z_5}{z_{45}^2} \left\{ U_4^{dd'} (U_5^{ee'} - U_4^{ee'}) \right. \\ &\times \left( \left[ 2I_1 - \frac{4}{z_{45}^2} \right] f^{ade} f^{bd'e'} (t^a U_1 t^b)_{ij} + \frac{(z_{14}, z_{15})}{z_{14}^2 z_{15}^2} \ln \frac{z_{14}^2}{z_{15}^2} \right. \\ &\times \left. \left. \left[ i f^{ad'e'} (\{t^d, t^e\} U_1 t^a)_{ij} - i f^{ade} (t^a U_1 \{t^{d'}, t^{e'}\})_{ij} \right] \right\} \\ &+ 8(t^a U_1 t^b)_{ij} n_f I_{f1} \text{tr} \{ t^a U_4 t^b (U_5^\dagger - U_4^\dagger) \} \\ &+ \frac{\alpha_s^2 N_c}{4\pi^3} \int \frac{d^2 z_4}{z_{14}^2} (U_4^{ab} - U_1^{ab}) (t^a U_1 t^b)_{ij} \\ &\times \left\{ \left[ \frac{11}{3} \ln z_{14}^2 \mu^2 + \frac{67}{9} - \frac{\pi^2}{3} \right] - \frac{n_f}{N_c} \left[ \frac{2}{3} \ln z_{14}^2 \mu^2 + \frac{10}{9} \right] \right\} \end{aligned} \quad (5)$$

where  $n_f$  is the number of active quark flavors and  $\mu$  is the normalization point. (The quark diagrams are similar to those in Fig. 2 a-d with the gluon loop replaced by the quark one). Hereafter we use the notations

$$\begin{aligned} I_1 &\equiv I(z_1, z_4, z_5) \\ &= \frac{\ln z_{14}^2 / z_{15}^2}{z_{14}^2 - z_{15}^2} \left[ \frac{z_{14}^2 + z_{15}^2}{z_{45}^2} - \frac{(z_{14}, z_{15})}{z_{14}^2} - \frac{(z_{14}, z_{15})}{z_{15}^2} - 2 \right], \end{aligned} \quad (6)$$

$I_2 \equiv I(z_2, z_4, z_5)$ , and

$$I_{f1} \equiv I_f(z_1, z_4, z_5) = \frac{2}{z_{45}^2} - \frac{2(z_{14}, z_{15})}{z_{14}^2 z_{15}^2 z_{45}^2} \ln \frac{z_{14}^2}{z_{15}^2} \quad (7)$$

(The integration variables are called  $z_4$  and  $z_5$  for uniformity of notations in all Sections).

The result in this form is correct both in fundamental and adjoint representations. (For quark contribution proportional to  $n_f$  one should replace  $t^a$  by adjoint representation matrices only in  $t^a U_1 t^b$  and leave the fundamental  $t^a$  and  $t^b$  in the quark loop). As we discussed in previous Section, this means that the results for the evolution of  $U^\dagger$  can be obtained by transposition. We have checked the “transposing rule” by explicit calculation.

### B. Pairwise interaction

The typical diagrams for pairwise interaction are shown in Fig. 2 c,d (and the full set is given by Fig. 6 in Ref. [6]) In this letter we present the final result, the details would be published elsewhere. The evolution equation for  $U \otimes U$  has the form

$$\begin{aligned} \frac{d}{d\eta}(U_1)_{ij}(U_2)_{kl} &= \frac{\alpha_s^2}{8\pi^4} \int d^2 z_4 d^2 z_5 (\mathcal{A}_1 + \mathcal{A}_2 + \mathcal{A}_3) \\ &+ \frac{\alpha_s^2 N_c}{8\pi^3} \int d^2 z_4 (\mathcal{B}_1 + \mathcal{B}_2) \end{aligned} \quad (8)$$

where the kernels  $\mathcal{A}_i(z_1, z_2, z_4, z_5)$  corresponds to diagrams of Fig.2 a,c type and  $\mathcal{B}_i(z_1, z_2, z_4)$  to Fig.2 b,d type. The explicit expressions are

$$\begin{aligned} \mathcal{A}_1 &= [(t^a U_1)_{ij}(U_2 t^b)_{kl} + (U_1 t^b)_{ij}(t^a U_2)_{kl}] \\ &\times \left[ f^{ade} f^{bd'e'} U_4^{dd'} (U_5^{ee'} - U_4^{ee'}) \right. \\ &\times \left( -K - \frac{4}{z_{45}^2} + \frac{I_1}{z_{45}^2} + \frac{I_2}{z_{45}^2} \right) \\ &\left. + 4n_f (I_{f1} + I_{f2} + K_f) \text{tr} \{ t^a U_4 t^b (U_5^\dagger - U_4^\dagger) \} \right] \end{aligned} \quad (9)$$

$$\begin{aligned} \mathcal{A}_2 &= 4(U_4 - U_1)^{dd'} (U_5 - U_2)^{ee'} \\ &\left\{ i [f^{ad'e'} (t^d U_1 t^a)_{ij} (t^e U_2)_{kl} \right. \\ &- f^{ade} (t^a U_1 t^{d'})_{ij} (U_2 t^{e'})_{kl}] J_{1245} \ln \frac{z_{14}^2}{z_{15}^2} \\ &+ i [f^{ad'e'} (t^d U_1)_{ij} (t^e U_2 t^a)_{kl} - f^{ade} (U_1 t^{d'})_{ij} (t^a U_2 t^{e'})_{kl}] \\ &\left. \times J_{2154} \ln \frac{z_{24}^2}{z_{25}^2} \right\} \end{aligned} \quad (10)$$

$$\begin{aligned} \mathcal{A}_3 &= 2U_4^{dd'} \left\{ i [f^{ad'e'} (U_1 t^a)_{ij} (t^d t^e U_2)_{kl} \right. \\ &\left. - f^{ade} (t^a U_1)_{ij} (U_2 t^e t^{d'})_{kl}] \right. \\ &\times \left[ J_{1245} \ln \frac{z_{14}^2}{z_{15}^2} + (J_{2145} - J_{2154}) \ln \frac{z_{24}^2}{z_{25}^2} \right] (U_5 - U_2)^{ee'} \\ &+ i [f^{ad'e'} (t^d t^e U_1)_{ij} (U_2 t^a)_{kl} - f^{ade} (U_1 t^e t^{d'})_{ij} (t^a U_2)_{kl}] \\ &\left. \times \left[ J_{2145} \ln \frac{z_{24}^2}{z_{25}^2} + (J_{1245} - J_{1254}) \ln \frac{z_{14}^2}{z_{15}^2} \right] (U_5 - U_1)^{ee'} \right\} \end{aligned} \quad (11)$$

for  $\mathcal{A}_i$  kernels and

$$\begin{aligned} \mathcal{B}_1 &= 2 \ln \frac{z_{14}^2}{z_{12}^2} \ln \frac{z_{24}^2}{z_{12}^2} \\ &\times \left\{ (U_4 - U_1)^{ab} i [f^{bde} (t^a U_1 t^d)_{ij} (U_2 t^e)_{kl} \right. \\ &+ f^{ade} (t^e U_1 t^b)_{ij} (t^d U_2)_{kl}] \left[ \frac{(z_{14}, z_{24})}{z_{14}^2 z_{24}^2} - \frac{1}{z_{14}^2} \right] \\ &+ (U_4 - U_2)^{ab} i [f^{bde} (U_1 t^e)_{ij} (t^a U_2 t^d)_{kl} \\ &+ f^{ade} (t^d U_1)_{ij} (t^e U_2 t^b)_{kl}] \left[ \frac{(z_{14}, z_{24})}{z_{14}^2 z_{24}^2} - \frac{1}{z_{24}^2} \right] \left. \right\} \end{aligned} \quad (12)$$

$$\begin{aligned} \mathcal{B}_2 &= [2U_4^{ab} - U_1^{ab} - U_2^{ab}] \\ &\left\{ \frac{(z_{14}, z_{24})}{z_{14}^2 z_{24}^2} \left[ \left( \frac{11}{3} - \frac{2n_f}{3N_c} \right) \ln z_{12}^2 \mu^2 + \frac{67}{9} - \frac{\pi^2}{3} - \frac{10n_f}{9N_c} \right] \right. \\ &+ \left. \left( \frac{11}{3} - \frac{2n_f}{3N_c} \right) \left( \frac{1}{2z_{14}^2} \ln \frac{z_{24}^2}{z_{12}^2} + \frac{1}{2z_{24}^2} \ln \frac{z_{14}^2}{z_{12}^2} \right) \right\} \\ &\times [(t^a U_1)_{ij} (U_2 t^b)_{kl} + (U_1 t^b)_{ij} (t^a U_2)_{kl}] \end{aligned} \quad (13)$$

for  $\mathcal{B}_i$  kernels. Here we used the following notations

$$\begin{aligned} J_{1245} &\equiv J(z_1, z_2, z_4, z_5) = \\ &\frac{(z_{14}, z_{25})}{z_{14}^2 z_{25}^2 z_{45}^2} - 2 \frac{(z_{15}, z_{45})(z_{15}, z_{25})}{z_{14}^2 z_{15}^2 z_{25}^2 z_{45}^2} + 2 \frac{(z_{25}, z_{45})}{z_{14}^2 z_{25}^2 z_{45}^2}, \end{aligned} \quad (14)$$

### C. Triple interaction

The diagrams for triple interaction are shown in Fig. 2 e,f (plus permutations). The result is

$$\begin{aligned}
\mathcal{J}_{1245} &\equiv \mathcal{J}(z_1, z_2, z_4, z_5) \\
&= \frac{(z_{24}, z_{25})}{z_{24}^2 z_{25}^2 z_{45}^2} - \frac{2(z_{24}, z_{45})(z_{15}, z_{25})}{z_{24}^2 z_{25}^2 z_{15}^2 z_{45}^2} \\
&+ \frac{2(z_{25}, z_{45})(z_{14}, z_{24})}{z_{14}^2 z_{24}^2 z_{25}^2 z_{45}^2} - \frac{2(z_{14}, z_{24})(z_{15}, z_{25})}{z_{14}^2 z_{15}^2 z_{24}^2 z_{25}^2} \quad (15) \\
K &= \frac{1}{z_{45}^4} \left[ \frac{z_{14}^2 z_{25}^2 + z_{15}^2 z_{24}^2 - 4z_{12}^2 z_{45}^2}{z_{14}^2 z_{25}^2 - z_{15}^2 z_{24}^2} \ln \frac{z_{14}^2 z_{25}^2}{z_{15}^2 z_{24}^2} - 2 \right] \\
&+ \frac{1}{2} \left( \frac{z_{12}^4}{z_{14}^2 z_{25}^2 - z_{15}^2 z_{24}^2} \left[ \frac{1}{z_{14}^2 z_{25}^2} + \frac{1}{z_{24}^2 z_{15}^2} \right] \right. \\
&+ \left. \frac{z_{12}^2}{z_{45}^2} \left[ \frac{1}{z_{14}^2 z_{25}^2} - \frac{1}{z_{15}^2 z_{24}^2} \right] \right) \ln \frac{z_{14}^2 z_{25}^2}{z_{15}^2 z_{24}^2} \quad (16)
\end{aligned}$$

and

$$K_f = \frac{1}{z_{45}^4} \left[ -2 + \frac{z_{14}^2 z_{25}^2 + z_{15}^2 z_{24}^2 - z_{12}^2 z_{45}^2}{z_{14}^2 z_{25}^2 - z_{15}^2 z_{24}^2} \ln \frac{z_{14}^2 z_{25}^2}{z_{15}^2 z_{24}^2} \right] \quad (17)$$

The conformally invariant kernels  $K$  and  $K_f$  are parts of the NLO BK equation for dipole evolution.

Again, the result in this form is correct both in fundamental and adjoint representations so the evolution of  $U \otimes U^\dagger$  and  $U^\dagger \otimes U^\dagger$  can be obtained by transposition of Eqs. (9-13). If one transposes Wilson line proportional to  $U_2$  in the l.h.s and r.h.s. of Eq. (8), takes trace of Wilson lines and adds self-interaction terms for  $U$  and  $U^\dagger$ , one reproduces after some algebra the NLO BK equation from Ref. [6]. (In doing so one can use the integral (20) below with replacements  $z_3 \rightarrow z_1$ ,  $z_1 \rightarrow z_2$  so that  $\mathcal{J}_{22145} = \mathcal{J}_{1245}$  and  $z_2 \rightarrow z_1$ ,  $z_3 \rightarrow z_2$  which gives  $\mathcal{J}_{12145} = \mathcal{J}_{1245}$ .) It should be noted that, although we calculated all diagrams anew, the results for two Wilson lines with open indices can be restored from the contributions of the individual diagrams in Ref. [6] since color structure of these diagrams is obvious even with open indices.

$$\begin{aligned}
&\frac{d}{d\eta} (U_1)_{ij} (U_2)_{kl} (U_3)_{mn} \\
&= i \frac{\alpha_s^2}{2\pi^4} \int d^2 z_4 d^2 z_5 \left\{ \mathcal{J}_{12345} \ln \frac{z_{34}^2}{z_{35}^2} \right. \\
&\times f^{cde} [(t^a U_1)_{ij} (t^b U_2)_{kl} (U_3 t^c)_{mn} (U_4 - U_1)^{ad} (U_5 - U_2)^{be} \\
&- (U_1 t^a)_{ij} (U_2 t^b)_{kl} (t^c U_3)_{mn} (U_4 - U_1)^{da} (U_5 - U_2)^{eb}] \\
&+ \mathcal{J}_{32145} \ln \frac{z_{14}^2}{z_{15}^2} \\
&\times f^{ade} [(U_1 t^a)_{ij} (t^b U_2)_{kl} (t^c U_3)_{mn} (U_4 - U_3)^{cd} (U_5 - U_2)^{be} \\
&- (t^a U_1)_{ij} \otimes (U_2 t^b)_{kl} (U_3 t^c)_{mn} (U_4^{dc} - U_3^{dc}) (U_5^{eb} - U_2^{eb})] \\
&+ \mathcal{J}_{13245} \ln \frac{z_{24}^2}{z_{25}^2} \\
&\times f^{bde} [(t^a U_1)_{ij} (U_2 t^b)_{kl} (t^c U_3)_{mn} (U_4 - U_1)^{ad} (U_5 - U_3)^{ce} \\
&- (U_1 t^a)_{ij} (t^b U_2)_{kl} (U_3 t^c)_{mn} (U_4 - U_1)^{da} (U_5 - U_3)^{ec}] \quad (18)
\end{aligned}$$

where

$$\begin{aligned}
\mathcal{J}_{12345} &\equiv \mathcal{J}(z_1, z_2, z_3, z_4, z_5) = -\frac{2(z_{14}, z_{34})(z_{25}, z_{35})}{z_{14}^2 z_{25}^2 z_{34}^2 z_{35}^2} \\
&- \frac{2(z_{14}, z_{45})(z_{25}, z_{35})}{z_{14}^2 z_{25}^2 z_{35}^2 z_{45}^2} + \frac{2(z_{25}, z_{45})(z_{14}, z_{34})}{z_{14}^2 z_{25}^2 z_{34}^2 z_{45}^2} + \frac{(z_{14}, z_{25})}{z_{14}^2 z_{25}^2 z_{45}^2} \quad (19)
\end{aligned}$$

As usual, the results for the evolution of  $U \otimes U \otimes U^\dagger$  etc. can be obtained by transposition of color structures in Eq. (18)

The terms with two and one intersections with the shock wave coincide with Ref. [14]. When comparing the results for the diagrams with one intersection (of Fig. 2e type) to that in Ref. [14] the following integral is useful:

$$\begin{aligned}
&\int \frac{d^2 z_5}{\pi} \mathcal{J}_{12345} \ln \frac{z_{34}^2}{z_{35}^2} \\
&= \left\{ \frac{(z_{14}, z_{24})}{2z_{14}^2 z_{24}^2} \ln \frac{z_{23}^2}{z_{24}^2} \ln \frac{z_{23}^2}{z_{34}^2} - z_2 \leftrightarrow z_3 \right\} \quad (20) \\
&+ \left\{ \left[ \frac{(z_{14}, z_{24})(z_{24}, z_{34})}{z_{14}^2 z_{24}^2} - \frac{(z_{14}, z_{34})}{z_{14}^2} \right] \frac{1}{i\kappa_{23}} \right. \\
&\times \left[ \text{Li}_2 \left( \frac{(z_{24}, z_{34}) + i\kappa_{23}}{z_{24}^2} \right) - \text{Li}_2 \left( \frac{(z_{24}, z_{34}) - i\kappa_{23}}{z_{24}^2} \right) \right. \\
&+ \left. \left. \frac{1}{2} \ln \frac{z_{24}^2}{z_{34}^2} \ln \frac{(z_{23}, z_{24}) + i\kappa_{23}}{(z_{23}, z_{24}) - i\kappa_{23}} \right] + z_2 \leftrightarrow z_3 \right\}
\end{aligned}$$

where  $\kappa_{23} \equiv \sqrt{z_{24}^2 z_{34}^2 - (z_{24}, z_{34})^2}$  and  $\text{Li}_2$  is the dilogarithm (which cancels in the final result (18)).

Note that we calculated the evolution of Wilson lines in the light-like gauge  $p_2^\mu A_\mu = 0$ . To assemble the evolution of colorless operators one needs to combine these

equations and connect Wilson lines by segments at infinity. These gauge links at infinity do not contribute to the kernel both in  $p_2^\mu A_\mu = 0$  and Feynman gauge (note, however, that their contribution is the only non-vanishing one in  $p_1^\mu A_\mu = 0$  gauge). Indeed, in the leading order it is easy to see because gluons coming from gauge links have a restriction  $\alpha < e^\eta$  so the gluon connecting points  $x, y$  with  $x_+ = L \rightarrow \infty$  and  $z_+ = 0$  (inside the shock-wave) will contain the factor  $\exp(i\frac{p_\perp^2}{\alpha_s}L)$  which vanishes for  $L \rightarrow \infty$  and  $\alpha$  restricted from above. Similarly one can prove that gauge links at infinity do not contribute to the NLO kernel and therefore the description of the evolution in terms of separate Wilson lines in the  $p_2^\mu A_\mu = 0$  gauge does make sense.

## V. CONCLUSION

We have calculated the full hierarchy of evolution equations for Wilson-line operators in the next-to-leading approximation. Two remarks, however, are in order.

First, our “building blocks” for evolution of Wilson lines are calculated at  $d = 4$  ( $d_\perp = 2$ ) so they contain infrared divergencies at large  $z_4$  and/or  $z_5$ , even at the leading order. For the gauge-invariant operators like color dipole or color quadrupole one can use our  $d_\perp = 2$  formulas since all these IR divergencies should cancel. If, however, one is interested in the evolution of color combinations of Wilson lines (like for octet NLO BFKL [15]) some of the above kernels should be recalculated in  $d = 4 + \epsilon$  dimensions.

Second, the NLO evolution equations presented here are “raw” evolution equations for Wilson lines with rigid

cutoff (1). For example, in  $\mathcal{N} = 4$  they lead to evolution equations for color dipole which is non-conformal. The reason (discussed in Ref. [7]) is that the cutoff (1) violates conformal invariance so we need an  $O(\alpha_s)$  counterterm to restore our lost symmetry. For the color dipole such counterterm was found in Ref. [7] and the obtained evolution for “composite conformal dipole” is Möbius invariant and agrees with NLO BFKL kernel for two-reggeon Green function found in Ref [16]. Thus, if one wants to use our NLO hierarchy for colorless objects such as quadrupole in  $\mathcal{N} = 4$  SYM one should correct our rigid-cutoff quadrupole with counterterms which should make the evolution equation for “composite conformal quadrupole” Möbius invariant. We hope to return to the quadrupole evolution in future publications. Another example is the evolution of the three quark Wilson lines  $\epsilon_{mnl}\epsilon_{m'n'l'}U_1^{mm'}U_2^{mm'}U_3^{mm'}$  (there are both pomeron and odderon contributions to this operator). After subtracting the Ref. [7] counterterms the NLO evolution equation for this operator becomes semi-invariant just as NLO BK in QCD [17]. The study is in progress.

## Acknowledgements

The authors are grateful to A. Grabovsky, H. Weigert and M. Lublinsky for valuable discussions. This work was supported by contract DE-AC05-06OR23177 under which the Jefferson Science Associates, LLC operate the Thomas Jefferson National Accelerator Facility and by U.S. Department of Energy under Grant No. de-sc0004286.

## References

- 
- [1] I. Balitsky, “*High-Energy QCD and Wilson Lines*”, [hep-ph/0101042]
  - [2] I. Balitsky, “*High-Energy Amplitudes in the Next-to-Leading Order*”, arXiv:1004.0057 [hep-ph]
  - [3] I. Balitsky, *Phys. Rev.* **D60**, 014020 (1999).
  - [4] I. Balitsky, *Nucl. Phys.* **B463**, 99 (1996); “*Operator expansion for diffractive high-energy scattering*”, [hep-ph/9706411];
  - [5] Yu.V. Kovchegov, *Phys. Rev.* **D60**, 034008 (1999); *Phys. Rev.* **D61**,074018 (2000).
  - [6] I. Balitsky and G.A. Chirilli, *Phys.Rev.* **D77**, 014019(2008)
  - [7] I. Balitsky and G.A. Chirilli, *Nucl. Phys.* **B822**, 45 (2009).
  - [8] I. Balitsky, *Phys.Rev.* **D75**, 014001 (2007).
  - [9] Yu. V. Kovchegov and H. Weigert, *Nucl. Phys.* **A784**, 188 (2007); *Nucl.Phys.* **A789**, 260(2007).
  - [10] A. Kovner and M. Lublinsky, *JHEP* **0611**, 083 (2006); A. Kovner and M. Lublinsky and a Weigert, *Phys.Rev.* **D74**, 114023 (2006); F. Dominguez, C. Marquet, A. Stasto, and Bo-Wen Xiao, *Phys.Rev.* **D87** 3, 034007 (2013), E. Iancu and D.N. Triantafyllopoulos, *JHEP***1311**, 067 (2013).
  - [11] I. Balitsky and G.A. Chirilli, *Phys.Rev.* **D83**, 031502 (2011), *Phys.Rev.* **D87**, 014013 (2013).
  - [12] J. Jalilian Marian, A. Kovner, A.Leonidov and H. Weigert, *Nucl. Phys.* **B504**, 415 (1997), *Phys. Rev.* **D59**, 014014 (1999); J. Jalilian Marian, A. Kovner and H. Weigert, *Phys. Rev.* **D59**, 014015 (1999); A. Kovner and J.G. Milhano, *Phys. Rev.* **D61**, 014012 (2000); A. Kovner, J.G. Milhano and H. Weigert, *Phys. Rev.* **D62**, 114005 (2000); H. Weigert, *Nucl. Phys.* **A703**, 823 (2002); E.Iancu, A. Leonidov and L. McLerran, *Nucl. Phys.* **A692**, 583 (2001), *Phys. Lett.* **B510**, 133 (2001); E. Ferreira, E. Iancu, A. Leonidov, L. McLerran, *Nucl. Phys.* **A703**, 489 (2002).
  - [13] A. Kovner, M. Lublinsky and Y. Mulian, *Complete JIMWLK Evolution at NLO*, e-print arXiv:1310.0378
  - [14] A.V. Grabovsky, *JHEP* **1309**, 141(2013)
  - [15] V.S. Fadin and L.N. Lipatov, *Phys.Lett.* **B706**, 470 (2012).
  - [16] V.S. Fadin, R. Fiore and A.V. Grabovsky, *Nucl.Phys.* **B831**, 248 (2010).
  - [17] I. Balitsky and A.V. Grabovsky, in preparation.